LETTER TO THE EDITOR

Brain
Pathology

Loss of fidelity in scanned digital images compared to glass slides of brain tumors resected using cavitron ultrasonic surgical aspirator

Abstract

Conversion of glass slides to digital images is necessary to capitalize on advances in computational pathology and could potentially transform our approach to primary diagnosis, research, and medical education. Most slide scanners have a limited maximum scannable area and utilize proprietary tissue detection algorithms to selectively scan regions that contain tissue, allowing for increased scanning speed and reduced file size compared to scanning the entire slide at high resolution. However, very small and faintly stained tissue fragments may not be recognized by these algorithms, leading to loss of fidelity in the digital image compared to the glass slides. Cavitron ultrasonic surgical aspirator (CUSA) is frequently used in brain tumor resections, resulting in highly fragmented specimens that are used for primary diagnosis. Here we evaluated the rate of loss of fidelity in 296 digital images from 40 CUSA-resected brain tumors scanned using a Philips Ultra Fast Scanner. Overall, 54% of the slides (at least one from every case) showed loss of fidelity, with at least one tissue fragment not scanned at high resolution. The majority of the missed tissue fragments were small (<0.5 mm), but rare slides were missing fragments greater than 5 mm in greatest dimension. In addition, 19% of the slides with missing tissue showed no indication of loss of fidelity in the digital image itself; the missing tissue could only be appreciated upon review of the glass slides. These results highlight a potential liability in the use of digital images for primary diagnosis in CUSA-resected brain tumor specimens.

Digital pathology presents tremendous opportunities to advance the clinical, research, and educational missions of academic pathology (1). A key first step in transitioning to a digital platform is conversion of glass slides to digital whole-slide images (WSI). To improve scanning speed and reduce file size, many companies have developed proprietary algorithms to detect tissue fragments and selectively scan only the identified regions of interest (ROI) at high resolution. This approach poses a risk of not scanning all of the tissue present on the glass slide, particularly small fragments, low-contrast staining tissue, and tissue located outside the manufacturer's recommended maximum scannable area (MSA). This is particularly concerning for neuropathology specimens given that focal findings (e.g., focal increase in mitotic activity, microvascular proliferation, necrosis, primitive neuronal component, etc.) can significantly impact tumor grading. Current guidelines from the College of American Pathologists (CAP) and the Food and Drug Administration (FDA) place the burden of responsibility on individual pathologists and pathology laboratories to perform validation studies to confirm that all of the material present on a glass slide is included in the digital image (2,3).

Brain tumor specimens are often omitted or included in very low numbers in digital pathology validation studies (4). In particular, brain tumors resected using cavitron ultrasonic surgical aspirator (CUSA), a surgical tool used frequently in brain tumor resections due to its lower risk of bleeding and other complications (5,6), are highly fragmented and may be particularly prone to scan infidelity. To assess the rate and extent of scan infidelity in CUSA-resected brain tumor specimens, we performed a retrospective study comparing glass slides and WSI. A total of 296 slides from forty cases were included: Twenty consecutive cases with CUSA material were selected from 2016 (n = 144 slides) and 20 were selected from 2018 (n = 152 slides). Between these two time frames, our department implemented various tissue processing modifications in preparation for digital sign-out, consistent with the FDA recommendations for use of

Philips IntelliSite Pathology Solution (PIPS), including submitting less tissue per cassette, using smaller molds for tissue embedding, discontinuing multiple "ribbon" sections per slide, and additional training for gross room and histology lab staff. The diagnoses included glioblastoma (n = 19 cases), anaplastic astrocytoma (n = 1 case), anaplastic oligodendroglioma (n = 4 cases), oligodendroglioma (n = 5 cases), diffuse astrocytoma (n = 7 cases), pilocytic astrocytoma (n = 2 cases), gliosis and focal cortical dysplasia (n = 1 case), and metastatic adenocarcinoma (n = 1 case).

Formalin-fixed paraffin-embedded CUSA material was sectioned at 4 μm and stained with hematoxylin and eosin. Slides were scanned using a Philips Ultra Fast Scanner (PIPS) at 0.25 μm per pixel resolution, equivalent to a 40× objective. The PIPS software first generates a low-resolution macro image of the entire slide, and then uses proprietary tissue detection algorithms to identify ROIs which are then tile-scanned at high resolution. The focal point is also determined automatically; additional information about these algorithms are not publicly available and the settings cannot be modified, to our knowledge.

The WSI and corresponding glass slides were reviewed independently by two neuropathologists (C.R.C. and M.P.) in a random order using PIPS (IMS 3.2) on a standard computer workstation (8GB RAM) with 27″ monitors (screen resolution 1920 × 1200) as recommended (3), and an Olympus BX42 microscope equipped with a standard set of objectives including a Uplan FL 40×. Only the CUSA-resected material from each case was evaluated. Small collections of Floseal, red blood cells or fibrin were not counted as tissue fragments. Statistical analyses were performed using custom-written Matlab-based software which is available, along with our entire dataset, at https://github.com/crcadwell/CUSA.

Overall, 54.1% (160/296) of the slides examined had at least one tissue fragment that was not scanned at high resolution in the WSI, including at least one slide from each case (range 3–8 slides/case). In the majority of WSI with infidelity (108/160, 67.5%), the missing tissue was less than 0.5 mm in greatest dimension; however, about a third (52/160, 32.5%) were missing fragments larger than 0.5 mm and rare slides (2/160, 1.3%) were missing fragments greater than 5 mm (Figure 1A–C). There was no difference in the rate of infidelity between the 2016 and 2018 cohorts (n = 81/144 [56.3%] for 2016, n = 79/152 [52.0%] for 2018; p = 0.49, Fisher's exact test). None of the unscanned tissue fragments would have altered the final diagnosis or grade.

PIPS defines the MSA as the center of the slide, 5 mm from the slide label and 3 mm from all other edges of the coverslip, corresponding to an area of 42 × 18 mm (760 mm^2; Figure 1D). Unscanned tissue outside this region was attributed to MSA restriction. ROIs could be either within the MSA or beyond it, and there could be multiple ROIs per slide. Unscanned tissue within the MSA was attributed to ROI selection, and slides with multiple unscanned

fragments could be attributed to a combination of ROI and MSA. Across all slides with unscanned tissue, the vast majority were attributed to ROI selection alone (137/160, 85.6%; Figure 1E), with a smaller number attributed to ROI + MSA (13/160, 8.1%) or MSA alone (10/160, 6.3%). Many of the small unscanned fragments were dispersed away from the main tissue bulk, and similar sized small fragments within the main bulk of tissue aggregate were successfully scanned. Although ROI was the most common cause of scan infidelity for both small and large fragments, it accounted for a greater fraction of the small unscanned fragments (97/108 or 89.8% for small fragments <0.5 mm; 39/52 or 75.0% for large fragments ≥0.5 mm; p = 0.0185, Fisher's exact test), whereas MSA alone accounted for a greater fraction of the large unscanned fragments (13.5% [7/52] for large fragments; 2.8% [3/108] for small fragments; p = 0.0141, Fisher's exact test; Figure 1F).

Loss of scan fidelity could be easily appreciated upon review of the WSI in instances where large fragments were abruptly cut off (e.g., Figure 1A). In some WSI, areas that are not scanned at high-resolution show blurry shadows on the macro-image that may raise suspicion for the presence of unscanned tissue. However, WSIs with multiple ROIs display solid white-out space between the scanned regions with no indication whether there may be unscanned tissue in these spaces (Figure 1G). For each slide we also determined whether the scanning infidelity could be identified on review of the WSI alone, or comparison with the glass slide was necessary, or a combination of both (Figure 1H). The vast majority of WSI with unscanned tissue fragments showed some indication that there may be unscanned tissue on the WSI (129/160 or 80.1%). Of these, about half showed additional unscanned fragments upon review of the glass slide that could not be appreciated on the WSI (63/129 or 48.8%). Of the slides with no indication of scanning infidelity on the WSI, nearly one in five showed unscanned tissue fragments upon review of the glass slide (31/167 or 18.6%). A comparison of the frequency of identification of small versus large unscanned tissue fragments on the WSI, glass, or both revealed that small fragments were more likely to be detected only on review of the glass slides compared to larger fragments of unscanned tissue (Figure 1I). Small fragments comprised the vast majority of instances in which the unscanned tissue could only be identified on the glass slide (n = 27/31 or 87.1%).

Our results highlight a limitation of the PIPS WSI system for the evaluation of fragmented brain specimens obtained using CUSA, with the majority of the loss of fidelity attributed to selective scanning of ROI which tends to miss small tissue fragments dispersed away from the main tissue aggregate. We found no evidence of improvement after optimizing our tissue processing protocols for slide scanning, suggesting that this technical shortcoming cannot be easily mitigated by such "hardware" modifications. As others have noted (7), review of the macro image along with the WSI can help to identify missed fragments; however,
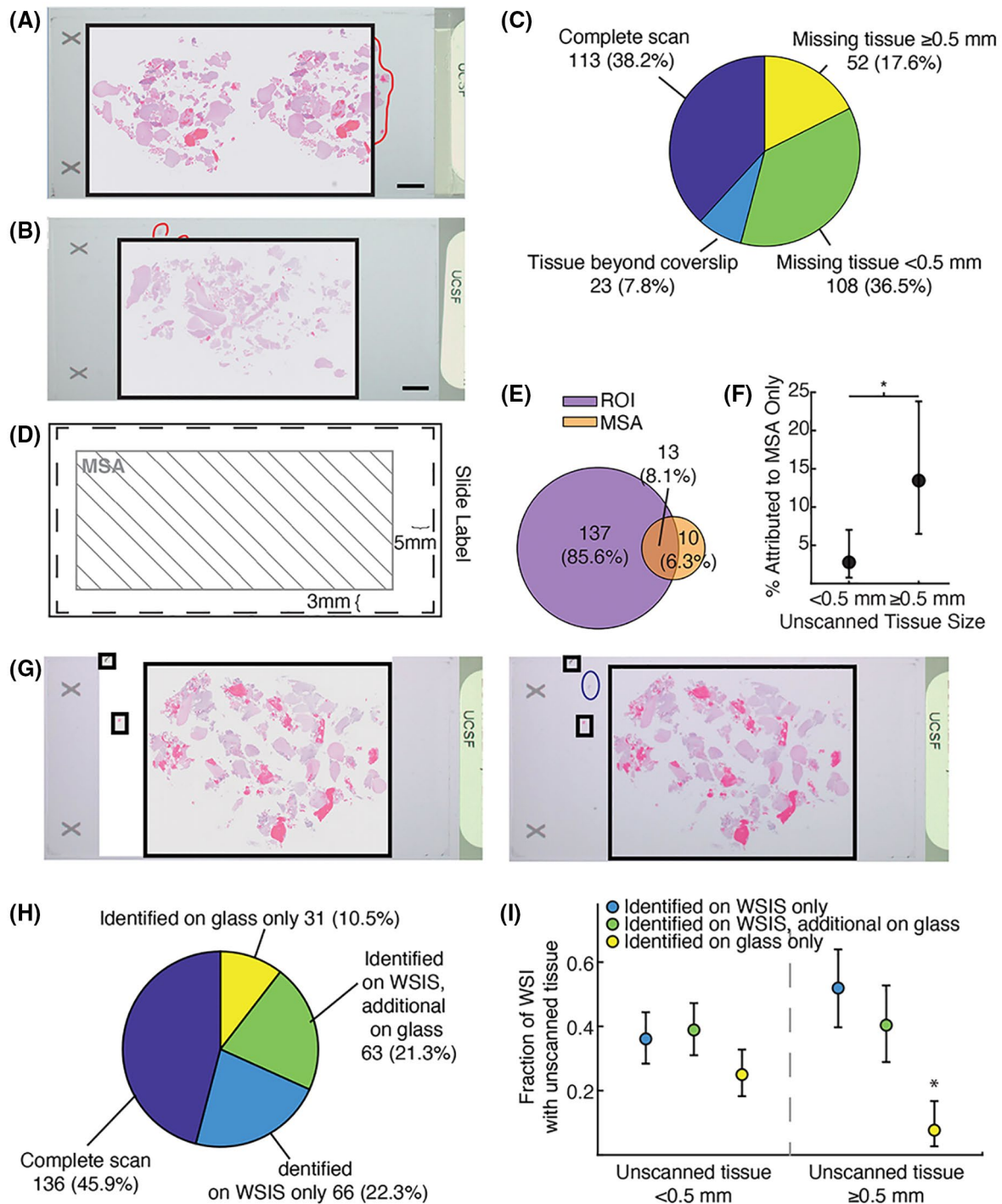
FIGURE 1 Loss of fidelity in scanned whole-slide images (WSI) is frequent and cannot always be appreciated without review of the glass slide. (A) Example WSI showing loss of fidelity with a large amount of unscanned tissue attributed to ROI selection. (B) Example WSI showing loss of fidelity, with multiple unscanned tissue fragments, attributed to a combination of ROI selection and MSA. (C) Summary of the frequency of infidelity (unscanned tissue) across all WSI examined (n = 296). Slides with missing tissue only beyond the coverslipped area were not counted as a loss of fidelity. (D) The manufacturer-defined the maximum scannable area (MSA, gray striped area) of each slide as the area at least 3mm from all edges of the coverslip (dashed line) and 5mm from the edge closest to the slide label. (E) Summary of the likely cause of infidelity (n = 160 WSI with unscanned tissue). (F) Percent of WSI with unscanned small (<0.5 mm) or large (>=0.5 mm) tissue fragments that are attributed to MSA only (n = 3/108 [2.8%] for small fragments and n = 7/53 [13.5%] for large fragments; *$p < 0.05$, Fisher's exact test). (G) Example WSI showing loss of fidelity with unscanned tissue that can only be detected on the glass slide. (H) Summary of the frequency of different modes of identification of scanning infidelity across all slides (n = 296). (I) Comparison of the frequency of different modes of identification of scanning infidelity between small and large unscanned tissue fragments (n = 39, 42, and 27 out of 108 total WSI with small unscanned tissue fragments, n = 27, 21, and 4 out of 52 total WSI with large unscanned tissue fragments; $p = 0.023$, overall χ^2 for 3 × 2 contingency table; post-hoc comparisons for each modality compared to the other two combined using χ^2 with Bonferroni correction for multiple comparisons; *$p < 0.05$ compared to the frequency of small unscanned fragments being detected on glass only). All stains are hematoxylin and eosin. In (A), (B) and (G), black boxes denote areas scanned at high resolution; red lines highlight unscanned fragments that could be seen on the WSI; blue ellipses indicate unscanned fragments that could only be seen on review of the glass slides; scale bars are 5 mm. Error bars in (F) and (I) are 90% Clopper-Pearson confidence intervals

review of the glass is still necessary to distinguish which are tissue and which are fibrin or debris and repeat scanning of a large fraction of slides would have significant impact on the workflow and turnaround time. Furthermore, a subset of slides with unscanned tissue (approximately 10% of all slides examined) could only be identified upon review of the glass slides.

A few studies evaluating WSI in diagnostic neuropathology have raised concerns such as loss of nuclear detail (8), but the main focus has been on diagnostic accuracy (9,10) and none have commented on scan fidelity. We evaluated a single WSI platform and the vast majority of our cases were gliomas; these results may not be representative of all platforms and neoplasms. Nonetheless, pathologists should be aware of the possibility of scan infidelity so that they can make an informed decision as to whether the benefits of digital pathology outweigh the potential risks. Novel tissue detection algorithms that emphasize scan fidelity over scanning speed may ultimately prove more efficient in clinical practice by reducing the number of cases requiring concurrent review of glass slides.

KEYWORDS
digital pathology, scanning infidelity, tissue detection, whole-slide image

CONFLICT OF INTEREST
The authors have no significant relationships with, or financial interest in, any commercial companies pertaining to this article.

AUTHOR CONTRIBUTIONS
All authors contributed to the study conception and design. Material preparation, data collection and analysis were performed by Cathryn R. Cadwell, Sarah Bowman and Melike Pekmezci. The first draft of the manuscript was written by Cathryn R. Cadwell and all authors commented on previous versions of the manuscript. All authors read and approved the final manuscript.

DATA AVAILABILITY STATEMENT
The data that support the findings of this study are available in the Supporting Information of this article.

Cathryn R. Cadwell
Sarah Bowman
Zoltan G. Laszik
Melike Pekmezci

Department of Pathology, University of California San Francisco, San Francisco, CA, USA

Correspondence
Melike Pekmezci, Department of Pathology, University of California San Francisco, 505 Parnassus Avenue, Suite M590, San Francisco, CA 94143-0511, USA.
Email: Melike.Pekmezci@ucsf.edu

ORCID
Cathryn R. Cadwell https://orcid.org/0000-0003-1963-8285
Melike Pekmezci https://orcid.org/0000-0003-2548-8359

REFERENCES
1. Madabhushi A, Lee G. Image analysis and machine learning in digital pathology: challenges and opportunities. Med Image Anal. 2016;33:170–5.
2. Pantanowitz L, Sinard JH, Henricks WH, Fatheree LA, Carter AB, Contis L, et al. Validating whole slide imaging for diagnostic purposes in Pathology: Guideline from the College of American Pathologists Pathology and Laboratory Quality Center. Arch Pathol Lab Med. 2013;137:1710–22.
3. United States Food and Drug Administration, Center for Devices and Radiological Health. Philips IntelliSite Pathology Solution (PIPS) Decision Summary (DEN no. 160056) 2017. Available at: https://www.accessdata.fda.gov/cdrh_docs/reviews/DEN160056.pdf. Accessed 8 January, 2021.
4. Mukhopadhyay S, Feldman MD, Abels E, Ashfaq R, Beltaifa S, Cacciabeve NG, et al. Whole Slide Imaging Versus Microscopy for Primary Diagnosis in Surgical Pathology: A Multicenter Blinded Randomized Noninferiority Study of 1992 Cases (Pivotal Study). Am J Surg Pathol. 2018;42:39–52.
5. Baddour HM, Lupa MD, Patel ZM. Comparing use of the Sonopet ® ultrasonic bone aspirator to traditional instrumentation during the endoscopic transsphenoidal approach in pituitary tumor resection. Int Forum of Allergy Rhinol. 2013;3:588–91.
6. Tang H, Zhang H, Xie Q, Gong Y, Zheng M, Wang D, et al. Application of CUSA excel ultrasonic aspiration system in resection of skull base meningiomas. Chin J Cancer Res. 2014;26:653–7.
7. Pekmezci M, Uysal SP, Orhan Y, Tihan T, Lee HS. Pitfalls in the use of whole slide imaging for the diagnosis of central nervous system tumors: A pilot study in surgical neuropathology. J Pathol Inform. 2016;7:25.
8. Fragetta F, Yagi Y, Garcia-Rojo M, Evans AJ, Tuthill JM, Baidoshvili A, et al. The importance of eSlide macro images for primary diagnosis with whole slide imaging. J Pathol Inform. 2018;9:46.
9. Alassiri A, Almutrafi A, Alsufiani F, Al Nehkilan A, Al Salim A, Musleh H, et al. Whole slide imaging compared with light microscopy for primary diagnosis in surgical neuropathology: a validation study. Ann Saudi Med. 2020;40(1):36–41.
10. Henriksen J, Kolognizak T, Houghton T, Cherne S, Zhen D, Cimino PJ, et al. Rapid validation of telepathology by an academic neuropathology practice during the COVID-19 pandemic. Arch Pathol Lab Med. 2020;144(11):1311–20. https://doi.org/10.5858/arpa.2020-0372-SA.

SUPPORTING INFORMATION
Additional Supporting Information may be found online in the Supporting Information section.